Resource

Cell Chemical Biology

# GFP-Aequorin Protein Sensor for Ex Vivo and In Vivo Imaging of $Ca^{2+}$ Dynamics in High-$Ca^{2+}$ Organelles

## Graphical Abstract

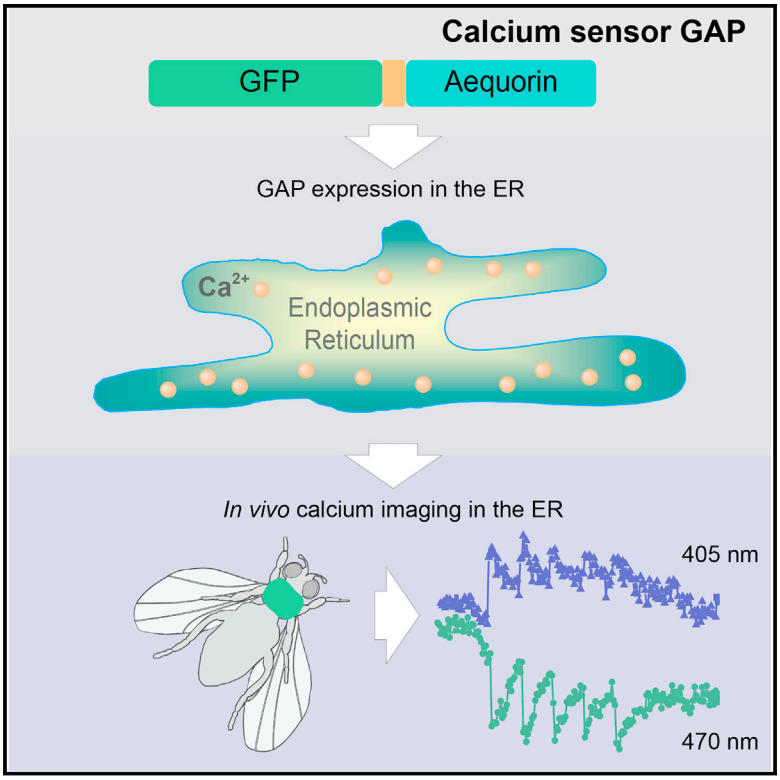


## Authors

Paloma Navas-Navarro, Jonathan Rojo-Ruiz, Macarena Rodriguez-Prados, María Dolores Ganfornina, Loren L. Looger, María Teresa Alonso, Javier García-Sancho

## Correspondence

talonso@ibgm.uva.es (M.T.A.), jgsancho@ibgm.uva.es (J.G.-S.)

## In Brief

Various organelles accumulate $Ca^{2+}$ at high concentrations required for their proper function. Navas-Navarro et al. developed a novel family of fluorescent sensors for imaging $Ca^{2+}$ in high [$Ca^{2+}$] organelles such as the ER. ER-targeted sensors enabled monitoring of ER $Ca^{2+}$ signals in vivo.

## Highlights

- A novel class of genetically encoded fluorescent $Ca^{2+}$ indicators is developed
- The new sensors are suitable for imaging $Ca^{2+}$ in organelles with high $Ca^{2+}$ levels
- They can be used to visualize $Ca^{2+}$ signals in the ER
- ER-targeted $Ca^{2+}$ sensors are successfully used to monitor ER $Ca^{2+}$ signals in vivo

## Accession Numbers

78118

Navas-Navarro et al., 2016, Cell Chemical Biology *23*, 1–8
June 23, 2016 
http://dx.doi.org/10.1016/j.chembiol.2016.05.010

CellPress

Please cite this article in press as: Navas-Navarro et al., GFP-Aequorin Protein Sensor for Ex Vivo and In Vivo Imaging of $Ca^{2+}$ Dynamics in High-$Ca^{2+}$ Organelles, Cell Chemical Biology (2016), http://dx.doi.org/10.1016/j.chembiol.2016.05.010

Cell Chemical Biology
Resource

# GFP-Aequorin Protein Sensor for Ex Vivo and In Vivo Imaging of $Ca^{2+}$ Dynamics in High-$Ca^{2+}$ Organelles

Paloma Navas-Navarro,[1,3] Jonathan Rojo-Ruiz,[1,3] Macarena Rodriguez-Prados,[1] María Dolores Ganfornina,[1] Loren L. Looger,[2] María Teresa Alonso,[1,*] and Javier García-Sancho[1,*]
[1]Instituto de Biología y Genética Molecular (IBGM), University of Valladolid and Consejo Superior de Investigaciones Científicas (CSIC), c/ Sanz y Forés 3, 47003 Valladolid, Spain
[2]Howard Hughes Medical Institute, Janelia Research Campus, Ashburn, VA 20147, USA
[3]Co-first author
*Correspondence: talonso@ibgm.uva.es (M.T.A.), jgsancho@ibgm.uva.es (J.G.-S.)
http://dx.doi.org/10.1016/j.chembiol.2016.05.010

## SUMMARY

**Proper functioning of organelles such as the ER or the Golgi apparatus requires luminal accumulation of $Ca^{2+}$ at high concentrations. Here we describe a ratiometric low-affinity $Ca^{2+}$ sensor of the GFP-aequorin protein (GAP) family optimized for measurements in high-$Ca^{2+}$ concentration environments. Transgenic animals expressing the ER-targeted sensor allowed monitoring of $Ca^{2+}$ signals inside the organelle. The use of the sensor was demonstrated under three experimental paradigms: (1) ER $Ca^{2+}$ oscillations in cultured astrocytes, (2) ex vivo functional mapping of cholinergic receptors triggering ER $Ca^{2+}$ release in acute hippocampal slices from transgenic mice, and (3) in vivo sarcoplasmic reticulum $Ca^{2+}$ dynamics in the muscle of transgenic flies. Our results provide proof of the suitability of the new biosensors to monitor $Ca^{2+}$ dynamics inside intracellular organelles under physiological conditions and open an avenue to explore complex $Ca^{2+}$ signaling in animal models of health and disease.**

## INTRODUCTION

Maintenance of high $[Ca^{2+}]$ in the lumen of $Ca^{2+}$-storage organelles, such as the ER or the Golgi apparatus (GO), is crucial for their correct functioning. Chronic decrease of $[Ca^{2+}]_{ER}$ triggers ER stress and the ''unfolded protein response'' (Gallego-Sandin et al., 2011), whereas reduction of $[Ca^{2+}]_{GO}$ disturbs segregation and cargo sorting (Kienzle and von Blume, 2014). Direct and calibrated measurements of intraluminal $Ca^{2+}$ levels are imperative to understand the $Ca^{2+}$ responses underlying different physiological and pathophysiological conditions. In the past decade an increasing number of genetically encoded $Ca^{2+}$ indicators (GECIs) have been developed. Most of them have been engineered to have high $Ca^{2+}$ affinity and only a few for use in high $[Ca^{2+}]$ environments (Henderson et al., 2015; Palmer and Tsien, 2006; Suzuki et al., 2014; Tang et al., 2011; Wu et al., 2014). Although some indicators have been expressed in transgenic animals, its utility has proven problematic, displaying small responses, probably due to the interaction of the sensor with endogenous partners. Furthermore, to date there are no reports on the in vivo use of transgenic low-$Ca^{2+}$ affinity indicators.

We have recently described a new family of fluorescent $Ca^{2+}$ sensors named GAP (GFP-aequorin protein) (Rodriguez-Garcia et al., 2014). A unique feature of this family is the use of aequorin instead of calmodulin or troponin-C to provide the $Ca^{2+}$-binding sites. This makes the association of the indicator with endogenous proteins (bio-orthogonality) much less likely thus avoiding possible interferences. Other advantages of the GAP sensors include its ratiometric capability and its targetability to various organelles. The first low-$Ca^{2+}$ affinity GAP variant, named GAP1, displays an apparent dissociation constant value for $Ca^{2+}$ ($K_D$) of 16 μM, much lower than other GECIs. GAP1 is valuable for measurement, for example, in the low-$Ca^{2+}$ subcompartment of the GO (Aulestia et al., 2015), but is still far below the resting $[Ca^{2+}]_{GO}$ in the high-$Ca^{2+}$ subcompartment or the $[Ca^{2+}]_{ER}$, which are in the range of 250–600 μM (Alonso et al., 1998; Aulestia et al., 2015).

We report the development of new low-$Ca^{2+}$ affinity sensors (GAP2 and GAP3) optimized for imaging $Ca^{2+}$ dynamics in vivo in high-$Ca^{2+}$ organelles. We demonstrate their use for $[Ca^{2+}]_{ER}$ monitoring under various experimental settings, including ER $Ca^{2+}$ oscillations in cultured astrocytes, ER $Ca^{2+}$ release by acetylcholine in hippocampal slices ex vivo, and sarcoplasmic reticulum (SR) $Ca^{2+}$ release in the muscle of transgenic flies in vivo.

## RESULTS AND DISCUSSION

### Optimization of GAP for Measuring in High $[Ca^{2+}]$ Environments

Because of its relatively high affinity for $Ca^{2+}$, the previously described ER-targeted GAP1 (erGAP1) only poorly detected small changes of $[Ca^{2+}]_{ER}$, although it was valuable for measurements of large variations in luminal $Ca^{2+}$ (Figure 1A). We therefore introduced new substitutions in the EF hands of aequorin to further decrease GAP affinity for $Ca^{2+}$. Of the 22 mutants tested (Supplemental Experimental Procedures), the double mutant D24N/D119A (named GAP2) displayed a $K_D$ of 407 μM

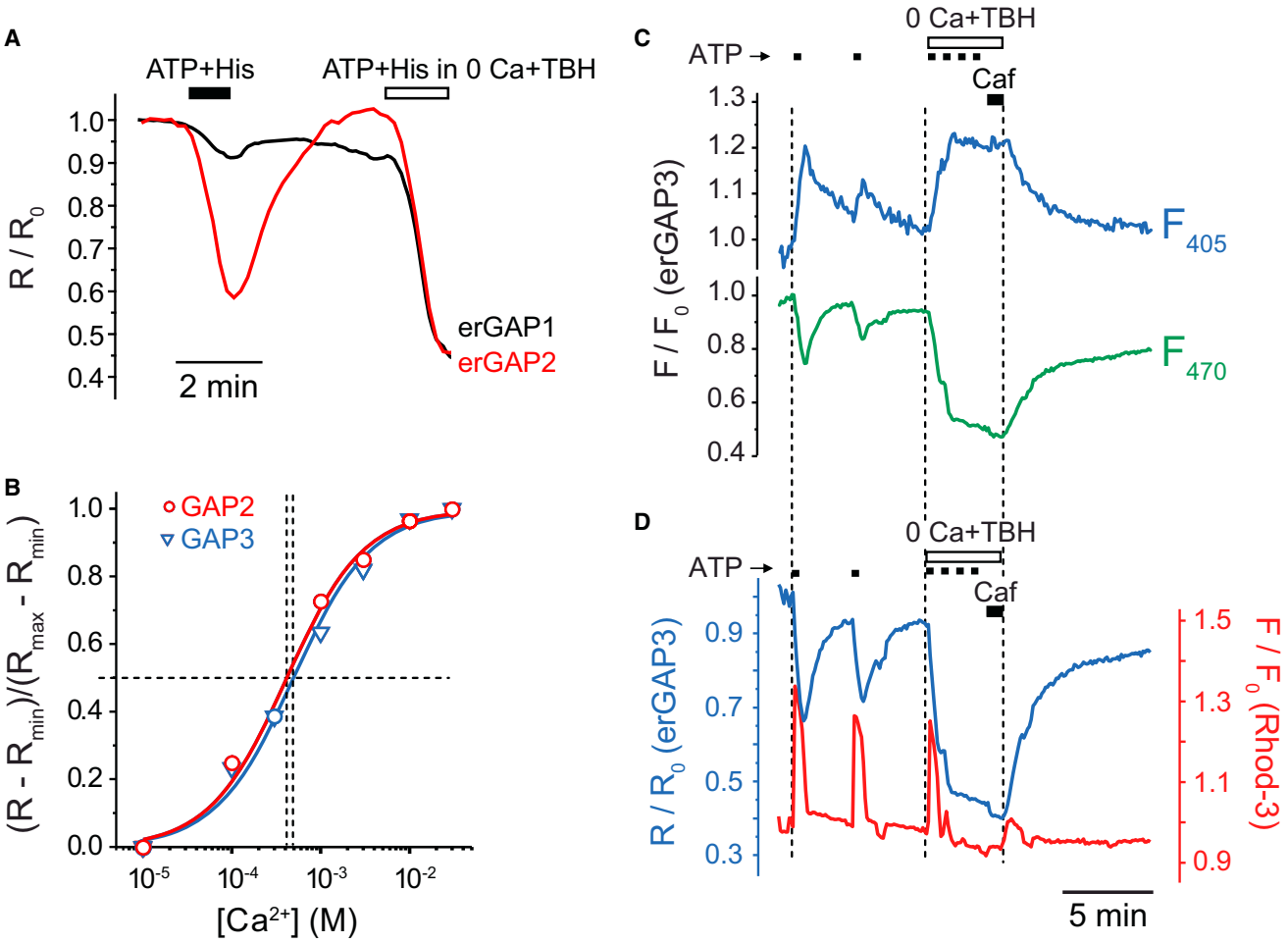


**Figure 1. Characterization of the New GAP Sensors**

(A) ER $Ca^{2+}$ emptying monitored with erGAP in HeLa cells. Comparison of the GAP1 and GAP2 submaximal responses to stimulation with ATP + histamine (100 μM each) followed by full ER emptying by stimulation with the same stimuli applied in $Ca^{2+}$-free medium containing 10 μM of the SERCA inhibitor TBH. Traces are the average of 22 (GAP1) or 11 (GAP2) cells. Experiments were performed in cell lines stably expressing either erGAP1 or erGAP2.

(B) Purified protein $Ca^{2+}$ titrations of GAP2 and GAP3; curves fit with Hill equation $y = (y_{max}[Ca^{2+}]^n)/(K_D^n + [Ca^{2+}]^n)$, yielding (mean ± SEM; n = 3): GAP2 $K_D$ = 407 ± 37 μM and n = 1.0 ± 0.1; GAP3 $K_D$ = 489 ± 43 μM and n = 0.9 ± 0.1.

(C) Response of erGAP3-expressing HeLa cells to repeated stimulation with ATP + carbachol (100 μM each; labelled as ATP), followed by response in $Ca^{2+}$-free medium containing 10 μM TBH; Caf, 50 mM caffeine. The trace is the average of 34 cells. Note the reciprocal changes of the individual fluorescence channels, $F_{470}$ and $F_{405}$.

(D) $F_{470}/F_{405}$ ratio (R) normalized to $R_0$ ($R/R_0$, in blue) is shown alongside simultaneous measurement of cytosolic $Ca^{2+}$ with Rhod-3 ($F/F_0$, in red).

See also Figures S1 and S2.

(Figure 1B), well suited for measuring $[Ca^{2+}]_{ER}$. As a consequence, the sensitivity of the improved ER-targeted GAP2 (erGAP2) to detect submaximal ER calcium releases was greatly increased with respect to erGAP1 (Figure 1A).

Further optimization of the indicator included humanization of GAP2 codon usage to improve expression in mammals and re-engineering of various residues in the GFP moiety to increase its fluorescence intensity (Supplemental Experimental Procedures). The brightest functional variant (named GAP3) contained the substitutions L15Q, I167V, S175G and D180Y and exhibited a $K_D$ of 489 μM. Importantly, the dynamic range (~3-fold) was not substantially altered with respect to the parental GAP1. Both GAP2 and GAP3 behaved very similarly and were used interchangeably in the following experiments. Remarkably, these sensors possess a Hill coefficient (n) of 1.0 (Figure 1B); it is likely that two out of the three $Ca^{2+}$-binding sites in aequorin have been rendered non-functional in GAP, while preserving the fluorescence signaling mechanism. Sensors with higher Hill coefficients are more difficult to calibrate (Suzuki et al., 2014). Furthermore, GAP is practically insensitive to variations in $Mg^{2+}$ concentration (in the 0.1–5 mM range; Figure S1A) or pH (in the 6.5–8.5 range; Figure S1B). At lower pH values the apparent affinity for $Ca^{2+}$ decreased (the $K_D$ increased 2.4 times at pH 6 and 40 times at pH 5.5; Figure S1B).

Accurate measurement of luminal $[Ca^{2+}]$ requires satisfaction of several criteria: high signal-to-noise ratio, large dynamic range

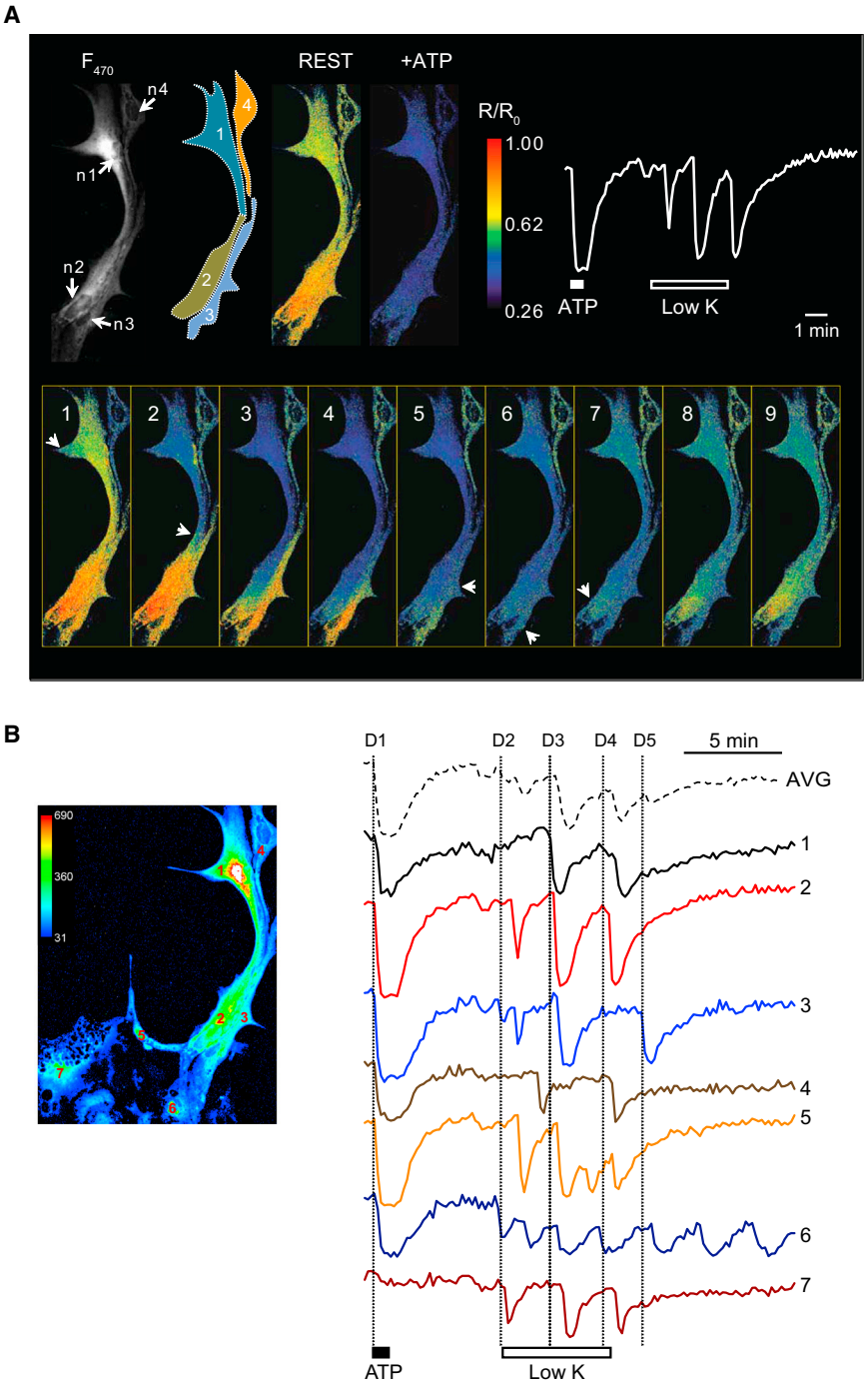


**Figure 2. Use of erGAP for Monitoring ER-$Ca^{2+}$ Oscillations in Cultured Astrocytes**

(A) Oscillations of $[Ca^{2+}]_{ER}$ induced by low $K^+$ (0.2 mM) in erGAP2-expressing astrocytes. The upper row shows a grayscale GAP fluorescence image in which four nuclei (n1–n4) can be seen. Next to it, the contours of the four cells and the pseudocolored ratio image at baseline (REST) and at maximum response with ATP (+ATP; 100 μM) are shown. The pseudocolor scale and the trace of cell 2 are shown at the right. Movie S1 shows the whole experiment. The lower row shows a series of nine images taken during one of the oscillations at a frame rate of one image every 10 s. Note that the $[Ca^{2+}]_{ER}$ drop starts in cell 1 (frame 1; start at the arrowhead), progresses toward cell 2 (frame 2; arrowhead), invades it (frames 3 and 4), and finally reaches cell 3 (frames 5 and 6). At frame 7, refilling of the ER calcium stores begins (at the arrowhead). Note that cell 4 oscillates independently. It is maximally depleted at frame 1 and refills during frames 2–9.

(B) Synchronization of ER $Ca^{2+}$ release during $Ca^{2+}$ oscillations in astrocytes. The same experiment as in (A) is shown. Regions of interest (ROI) (1–7) were defined in different cells as shown over the pseudocolored image, which is the average of all the images of the whole experiment. Ordinate: $R/R_0$ in a.u. Traces have been displaced vertically for better visibility. AVG, averaged value of the seven cells in the field. Note that $[Ca^{2+}]_{ER}$ decrease (D) is synchronous at D1 (ATP-induced), whereas D2–D5 start in one cell and then progress to the others.

See also Movie S1.

with a midpoint close to resting $[Ca^{2+}]$, and reliable in situ calibration. We targeted GAP3 to the ER (erGAP3); erGAP3 was bright and co-localized with ER markers. Cell stimulation with ATP plus carbachol produced large, coordinated changes in the fluorescences excited at 405 and 470 nm (Figure 1C). Complete emptying of the ER resulted in $F_{min}$, that was obtained by stimulation in $Ca^{2+}$-free medium containing the reversible sarco-ER $Ca^{2+}$ ATPase (SERCA) inhibitor tert-butylhydroquinone (TBH) (Moore et al., 1990) (Figure 1C). Similar results were obtained with the irreversible SERCA blocker thapsigargin (Thastrup et al., 1989), although in this case ER stores did not refill after inhibitor washout (Figure S2A). Finally, we calibrated erGAP3 response against the cytoplasmic $Ca^{2+}$-sensitive dye Rhod-3, whose red fluorescence was easily separable from GAP3 (Figure 1D, shown together with the erGAP3 $R/R_0$ ratio values). Interestingly, comparison of $Ca^{2+}$ kinetics in the two compartments revealed that the cytosolic $Ca^{2+}$ peak preceded the ER $Ca^{2+}$ decrease peak (Figure 1D). erGAP3 was also calibrated against Fura-2 (Figure S2B) with similar results. These findings indicate that $[Ca^{2+}]_C$ changes only crudely correlate with $[Ca^{2+}]_{ER}$ changes and direct ER measurements are required for precise description of $Ca^{2+}$ kinetics in this compartment.

## Oscillations of $[Ca^{2+}]_{ER}$ in Cultured Cortical Astrocytes

We next applied the new sensors to explore various aspects of ER $Ca^{2+}$ dynamics under three experimental paradigms. In the first setting we expressed the ER-targeted sensor in cortical astrocytes by infecting primary cultures with an erGAP2 herpes viral vector (Figure 2). The indicator successfully reported $[Ca^{2+}]_{ER}$ dynamics and was sensitive enough to

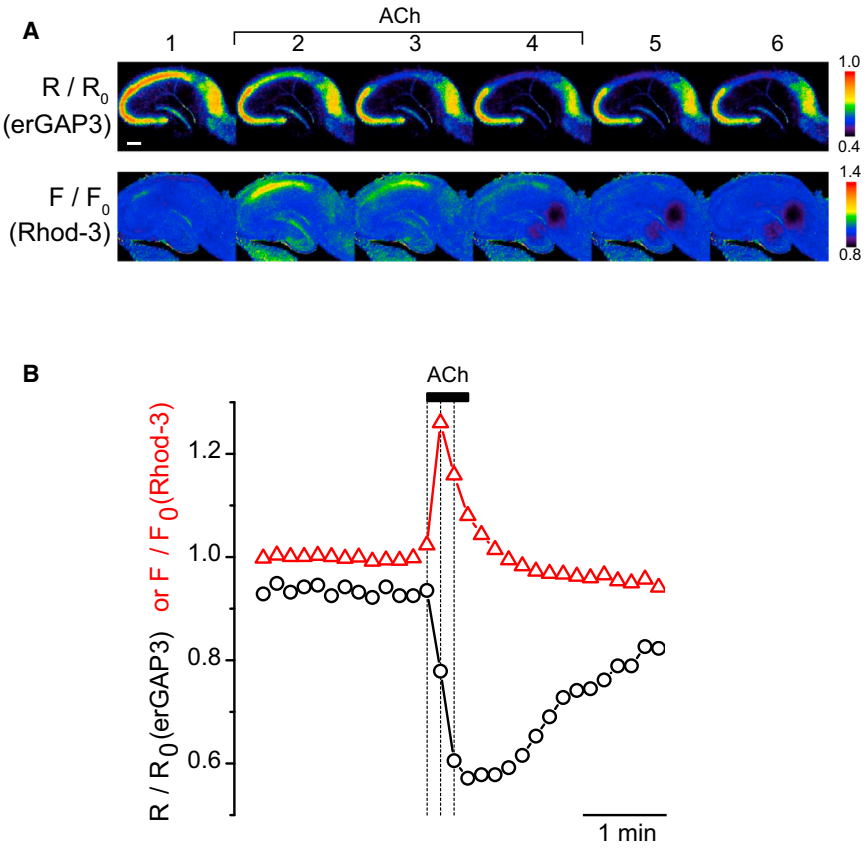


**Figure 3. Functional Mapping of Acetylcholine Responses in Hippocampal Slices Ex Vivo**

(A) Frame sequence during stimulation with acetylcholine (ACh; 200 μM, 30 s) in acute hippocampal slices from erGAP3 transgenic mice (line 10; P7). Cornus ammonis (CA) regions and the upper blade of dentate gyrus (DG) are visible. Measurements of ER $Ca^{2+}$ (erGAP3) and cytosolic $Ca^{2+}$ (Rhod-3) were performed simultaneously. Frames were acquired every 10 s. Upper row: ER $Ca^{2+}$ release, evidenced by the decrease of the GAP signal in CA1, during ACh stimulation. Calibration bar, 200 μm. Lower row, coordinated increase of Rhod-3 fluorescence, indicating the increase of $[Ca^{2+}]_C$ by release from the ER.

(B) Detailed kinetics of experiment shown in (A). Each graph symbol corresponds to 10 s. Note that the peak increase of $[Ca^{2+}]_C$ occurs 10 s after the application of ACh, whereas maximum $[Ca^{2+}]_{ER}$ decrease required more than 30 s. The relaxation of the $[Ca^{2+}]_C$ peak was also faster than that of the $[Ca^{2+}]_{ER}$ peak. Movie S2 shows the changes in erGAP3 along the whole experiment. Similar results were obtained with erGAP2 transgenic mice (line 3). See also Figure S3 and Movie S2.

follow $Ca^{2+}$ oscillations inside the ER. Stimulation with ATP, which induces $Ca^{2+}$ release from the ER via inositol trisphosphate (Verkhratsky et al., 2012), reduced the GAP fluorescence ($R/R_0$) by about 50% (Figure 2A). In these cells, low extracellular $[K^+]$ induces $Ca^{2+}$ entry and triggers oscillations of the cytosolic $Ca^{2+}$ (Dallwig et al., 2000). We demonstrate here that the cytosolic oscillations are due to large $[Ca^{2+}]_{ER}$ oscillations that could be directly recorded with erGAP2 (Movie S1). The entry of $Ca^{2+}$ across the plasma membrane would firstly trigger a $Ca^{2+}$ release from the ER via activation of the ryanodine receptor (RyR) through a process of $Ca^{2+}$-induced $Ca^{2+}$ release (Alonso et al., 1999). The luminal depletion will then desensitize the RyR and promote the gradual $Ca^{2+}$ loading of the ER. As soon as the luminal $Ca^{2+}$ reached a threshold, it would sensitize the RyR such that it started to release $Ca^{2+}$ again. These regular cycles of $Ca^{2+}$ release and uptake across the ER membrane will operate as long as the $Ca^{2+}$ flowing into the cell is guaranteed by the continuous low extracellular $[K^+]$ stimulation.

In addition, detailed analysis of the probe signal enabled us to investigate how $[Ca^{2+}]_{ER}$ oscillations are propagated from cell to cell. The lower panel in Figure 2A shows details of the cell-to-cell progression. It seems clear that cell excitation was able to spread from one cell to its neighbor and to trigger $Ca^{2+}$ release (arrowheads in Figure 2A). The main wave was visible in the average trace of all the cells present in the field (n = 7; Figure 2B), indicating some degree of synchronization.

## Functional Mapping of ER $Ca^{2+}$ Responses to Neurotransmitters in Hippocampal Slices Ex Vivo

We next generated lines of transgenic mice expressing erGAPs (2 and 3) under the ubiquitous *CAG-GS* promoter (Figure S3A). The hippocampus showed strong expression of the sensors (Figure S3B). We looked for functional responses to neurotransmitters in the different areas of the hippocampus examined at low magnification using acute slices from erGAP3 transgenic mice. ER $Ca^{2+}$ and cytosolic $Ca^{2+}$ dynamics were simultaneously monitored using erGAP3 and Rhod-3, respectively (Figure 3 and Movie S2). ER $Ca^{2+}$ release in response to acetylcholine selectively occurred in the CA1 region (Figure 3A). These results correlate well with the expression of the muscarinic acetylcholine receptors (Fernandez de Sevilla et al., 2008; Power and Sah, 2002). Interestingly, a detailed comparison between $[Ca^{2+}]_C$ and $[Ca^{2+}]_{ER}$ kinetics (Figure 3B) showed that maximal $[Ca^{2+}]_C$ rise preceded maximal ER release, in agreement with the results shown above in HeLa cells (Figure 1D).

## In Vivo Monitoring of $Ca^{2+}$ Release in the Sarcoplasmic Reticulum of Fly Muscle

To demonstrate the feasibility of in vivo measurements with the new ER $Ca^{2+}$ sensors, we genetically engineered *Drosophila* to express GAP3 specifically in the SR of striated muscles (Figures 4A and 4B). We investigated SR $Ca^{2+}$ dynamics in the living fly by imaging GAP fluorescence in the thorax muscles during electrical stimulation of the giant fiber, a useful model system for studies of muscle function during nerve stimulation that permits simultaneous activation of all the motor nerves (Allen and Godenschwege, 2010). At low frequency (0.25–0.5 Hz), GAP3 readily detected individual SR-release events secondary to nerve

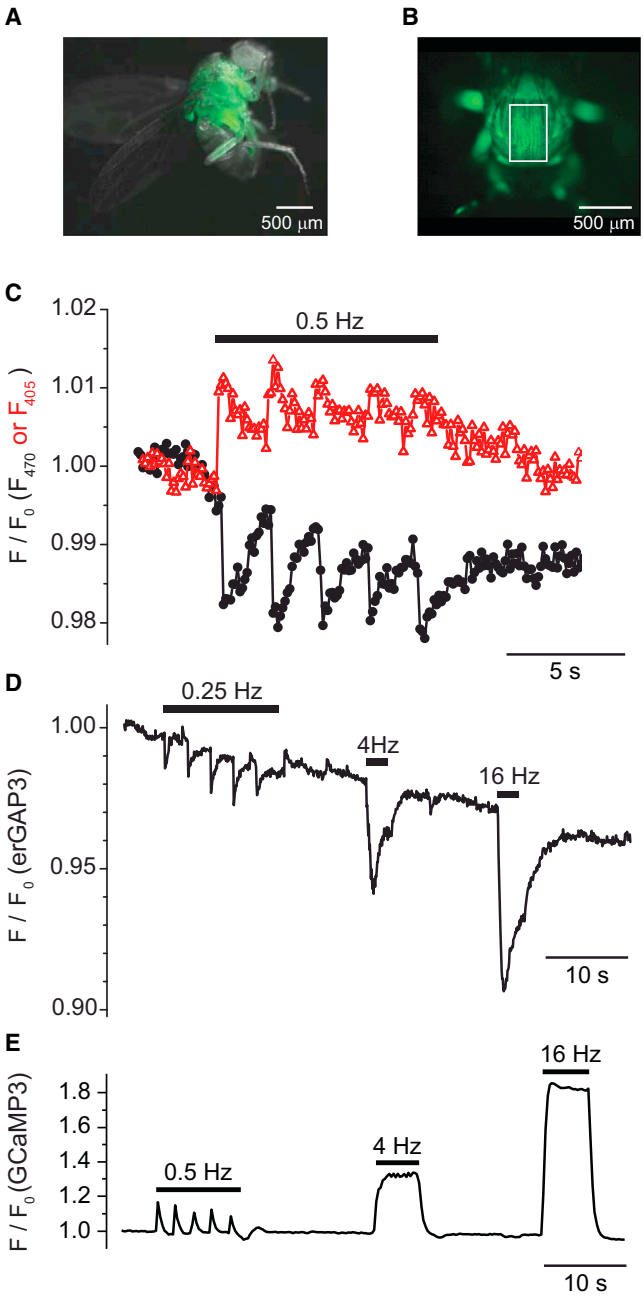


**Figure 4. Monitoring $[Ca^{2+}]_{ER}$ Dynamics during Muscle Contraction in the Living Fly with erGAP3**

(A and B) Specific expression of erGAP3 (green fluorescence) in the thoracic muscle of the *Mhc*-erGAP3 fly. Lateral views of bright field and fluorescence images are superimposed in (A). Dorsal views of fluorescence and the ROI images are shown in (B). The muscles were stimulated via the giant fiber (see Experimental Procedures) at different frequencies with 5–10 V/30–50 ms stimuli.

(C) Individual SR-release $Ca^{2+}$ events recorded on stimulation at low frequency (0.5 Hz). Reciprocal responses of the GAP3 fluorescence excited at 470 and 405 nm. Fluorescence images were acquired every 100 ms.

(D) Comparison of ER $Ca^{2+}$ release during stimulation at low- (0.25 Hz) and high-frequency (4 and 16 Hz). The traces of fluorescence excited at 470 nm are shown.

(E) Complementary changes in the cytosolic $Ca^{2+}$ ($F/F_0$), measured with GCaMP3.

See also Figure S4.

stimuli, with small and repetitive decreases in $F_{470}$ and concomitant rises in $F_{405}$ (Figure 4C). SR $Ca^{2+}$ release was completed in less than 100 ms and was followed by a slower $Ca^{2+}$ reuptake ($T_{1/2}$, 0.5–1 s) (Figures 4C and S4A). At high-frequency stimulation (4–16 Hz), individual SR-release events fused and peaked during the first 1.5 s, resulting in a much larger release (Figures 4D, S4B, and S4C). We also generated transgenic flies expressing GCaMP3 in muscle to image cytosolic $Ca^{2+}$ in parallel experiments. The decreases in $[Ca^{2+}]_{SR}$, imaged with GAP3, correlated well with the large increases in $[Ca^{2+}]_C$, imaged with GCaMP3 (Figure 4E). These results demonstrate that the new sensor erGAPs enable monitoring of SR-$Ca^{2+}$-release dynamics in response to physiological stimulation with a high temporal resolution in vivo.

The new sensors could also be targeted to specific subcompartments of the ER such as the nuclear envelope. Deep invaginations of the nuclear envelope within the nucleus expressing $InsP_3Rs$ form the so-called nucleoplasmic reticulum. Discrete release of $Ca^{2+}$ may selectively modulate nuclear calcium-regulated transcription (Alonso and Garcia-Sancho, 2011). Other subcompartments of the ER that could also be explored include ER membrane contact sites, both with the plasma membrane and with intracellular membranes of other organelles such as the lysosome or the mitochondria, where microdomains of high $Ca^{2+}$ have been proposed (Csordas et al., 2010; Giacomello et al., 2010). On the other hand, given the recent expansion of hues in fluorescent proteins (Shaner et al., 2004), future efforts will focus on the engineering of GAP variants with different colors (cyan, yellow, orange, or red) that enable simultaneous imaging of $Ca^{2+}$ in various locations. Fusions of aequorin to red fluorescent proteins such as mRFP1 (Manjarres et al., 2008) or td-tomato (Bakayan et al., 2011) have been previously reported as bioluminescent sensors. Substitution of the GFP moiety of GAP for mRFP1 rendered a protein insensitive to calcium (P.N.-N., unpublished data). An infrared sensor would be especially valuable for multiphoton microscopy and deeper imaging in scattering tissues.

In summary, the optimized $Ca^{2+}$ sensors represent a substantial improvement over previous GAPs due to its optimal $K_D$ for measurements in high $[Ca^{2+}]$ compartments, its ratiometric measurements, large dynamic range, and uncomplicated calibration (Rodriguez-Garcia et al., 2014). Even more relevant is its bio-orthogonal nature, which facilitates robust functional expression of the indicator with no apparent off-target effects. Finally, we demonstrate the applicability of the sensor, both ex vivo and in vivo, to address different aspects of subcellular $Ca^{2+}$ homeostasis. Its use in combination with new disease models, such as those provided by iPS cell technology (Fernandez-Santiago and Ezquerra, 2016; Wan et al., 2015), promises novel approaches to investigate the pathophysiological relevance of organellar $Ca^{2+}$ dyshomeostasis.

## SIGNIFICANCE

**Intracellular organelles such as the ER or the Golgi apparatus require luminal accumulation of $Ca^{2+}$ at high concentrations for proper functioning. Direct intra-organellar measurement of $Ca^{2+}$ concentrations in intact preparations is essential to address complex physiological questions.**

**Few genetically encoded $Ca^{2+}$ indicators have been developed for high-$Ca^{2+}$ organelles, and none of these have been used in vivo in the context of transgenic expression. We describe a new $Ca^{2+}$ sensor of the GFP-aequorin protein (GAP) family designed to accurately monitor $Ca^{2+}$ concentration in high-$Ca^{2+}$ environments. Expression of the sensor in the ER in neurons and muscle of transgenic animal models (flies and mice) enabled monitoring of fast physiological responses under minimally disturbing conditions ex vivo and in vivo. This sensor provides a valuable tool to explore subcellular complex $Ca^{2+}$ signaling in vivo in animal disease models.**

## EXPERIMENTAL PROCEDURES

### Gene Construction

The original GAP containing the D119A substitution in aequorin (Rodriguez-Garcia et al., 2014) was cloned in pcDNA3. The initial GAP gene library was constructed by site-directed mutagenesis (QuickChange Site-Directed Mutagenesis Kit; Stratagene) using oligonucleotides 1–22 (Supplemental Experimental Procedures). Genes encoding GAP variants were subcloned into pET28a for expression, purification, and screening in *Escherichia coli*. The secondary GAP library was created using erGAP2 cloned in pcDNA3 as a template and oligonucleotides 23–29 (Supplemental Experimental Procedures).

To target GAP2 or GAP3 to the ER (erGAP), the calreticulin signal peptide and the sequence encoding the ER-retention tag, KDEL, were fused in-frame to the 5′ and the 3′ end, respectively, resulting in pcDNA3-erGAP2 and pcDNA3-erGAP3. To produce viral vectors, erGAP2 cDNA was cleaved from pcDNA3 as a HindIII/EcoRI fragment and cloned into the herpes simplex virus plasmid pHSVpUC.

In order to improve gene expression in mice, sequence optimization of the erGAP2 gene was performed (ATG:biosynthetics). To make transgenic mice, mammalian codon use-optimized erGAP2 and erGAP3 were subcloned into the pCAG-GS vector with a *CAG* promoter (Miyazaki et al., 1989) (CMV enhancer, β-actin promoter) and regulatory elements from the woodchuck hepatitis virus (WPRE; Figure S3A). To make transgenic flies, erGAP3 was cloned into the pUASt-attB vector (GenBank: EF_362409). The integrity of all constructs was verified by sequencing.

### Bacterial Expression and Protein Purification

GAP variants in pET28a were transformed in *E. coli* BL21 (Stratagene). For protein expression, bacteria were grown at 37°C to $A_{600}$ >0.6 in Luria-Bertani medium containing 40 mg/l kanamycin and induced with 0.5 mM isopropyl β-D-thiogalactoside for 6 hr at 25°C. The cells were then pelleted by centrifugation at 6,000 × *g* for 10 min, and sonicated in a buffer containing 250 mM NaCl, 5 mM EDTA, 0.5 mM phenylmethylsulfonyl fluoride, 2 mM DTT (reducing agent), 50 mM Tris-HCl (pH 8.8). The bacterial lysate was centrifuged at 30,000 × *g* for 10 min. Most of the protein was present in inclusion bodies as an insoluble material that could be solubilized in 8 M urea, 5 mM DTT, 50 mM Tris-HCl (pH 8.8), by rocking at 4°C overnight. The insoluble protein was removed by centrifugation at 30,000 × *g* for 15 min. For small-scale cultures used for screening, protein in supernatant was refolded by filtration with 150 mM NaCl, 5 mM DTT, 50 mM Tris-HCl (pH 8.8) at 4°C using a 10K filter (Amicon) in such a way that urea was 125-fold diluted. For $Ca^{2+}$ titration of GAP2 or GAP3, urea was dialyzed against 50 mM Tris-HCl (pH 8.8) at 4°C. Next, 5 mM DTT was added and proteins were further purified with Ni-Sepharose beads (GE Healthcare). Protein quantification was performed using the Bradford method.

### GAP Screening

Mutant screening (Supplemental Experimental Procedures) was performed using a Tecan Genios Pro 96-well plate reader. GAP recombinant proteins (3 μg) were added to each well containing 200 μl of PBS (pH 7.4) at three different $Ca^{2+}$ concentrations: 0 (0.1 mM EGTA added), 0.1 mM, and 1 mM. GAP fluorescence was measured in triplicate at 390 and 485 nm excitation and 535 nm emission. These values were used to calculate the $F_{485}/F_{390}$ ratio (which was similar to the $F_{470}/F_{405}$ ratio). Ratio values obtained with $Ca^{2+}$ (0.1 and 1 mM $Ca^{2+}$) were divided by those obtained with EGTA ($R_{Ca}/R_{EGTA}$) and, finally, the values obtained with 1 mM $Ca^{2+}$ were divided by those obtained with 0.1 mM $Ca^{2+}$. Only those GAP mutants that gave $R_{Ca1}/R_{Ca0.1}$ values larger than 1.5 were pursued. The secondary screening of GAP2 mutants was performed in transiently transfected HeLa cells.

### Calibration with $Ca^{2+}$ and Interactions with $H^+$ and $Mg^{2+}$

Measurements were performed in the plate reader (see above). Recombinant GAP proteins (3 μg) were added to each well with 200 μl of a buffer containing 140 mM KCl, 1 mM $MgCl_2$, 20 mM MOPS/Tris (pH 7.2). $Ca^{2+}$ calibrations were performed in $Ca^{2+}$-free medium (0.1 mM EGTA added), or in the same solutions containing increasing $Ca^{2+}$ concentrations between 50 μM and 50 mM. $R_{max}$ and $R_{min}$ were computed as the $F_{485}/F_{390}$ ratios at saturating $[Ca^{2+}]$ and at zero $[Ca^{2+}]$, respectively. The $Ca^{2+}$ titration values fitted the Hill equation, $y = (y_{max}[Ca^{2+}]^n)/(K^n + [Ca^{2+}]^n)$, where y is $(R - R_{min})/(R_{max} - R_{min})$, K is the dissociation constant, $K_D$, and n is the Hill coefficient. The effects of pH were monitored with GAP2 using different buffers for each pH range: histidine for pH 5.5–6.5, MOPS/Na for pH 6.5–7.5, and Tris/HCl for pH 8–8.5. The effects of $Mg^{2+}$ were monitored by varying the added $MgCl_2$ between 0.1 and 5 mM.

### Cell Culture and Expression in Mammalian Cells

HeLa cells were maintained in DMEM (Invitrogen) supplemented with 10% fetal bovine serum, 2 mM L-glutamine, 100 μg/ml streptomycin, and 100 U/ml penicillin. Stable HeLa clones expressing erGAP2 or erGAP3 were obtained by lipofectamine transfection followed by G-418 selection. The population of GFP-positive cells was enriched by cell sorting. Single-cell clones were selected in culture medium containing 0.8 mg/ml G-418 by limited dilution and maintained in 0.1 mg/ml G-418. For imaging experiments, 5 × $10^4$ cells were seeded on poly-L-lysine-coated 12 mm diameter coverslips.

### Cortical Astrocyte Cultures

Brain cortices were dissected from three P2-3 C57BL/6JCrl (Charles Rivers) mice in cold Hank's balanced salt solution (HBSS) and digested with 0.5 mg/ml papain and 0.04 mg/ml DNase dissolved in a $Ca^{2+}$-free and $Mg^{2+}$-free HBSS with 10 mM glucose and 0.1% BSA at 37°C for 20 min. The cells were resuspended with minimal essential medium supplemented with 2 mM glutamax, 27 mM glucose, 100 μg/ml streptomycin, 100 U/ml penicillin, and 10% (v/v) horse serum, and plated on a poly-L-lysine-coated 75 $cm^2$ flask. After 2 and 7 days flasks were slapped to remove neurons and other loosely attached cells such as microglia and oligodendrocytes. After 1 week, cells were trypsinized and seeded in the same medium onto poly-L-lysine-coated 12 mm diameter glass coverslips at a density of 2.5 × $10^4$ cells/coverslip. The cultures were used within 1–2 weeks.

### Virus Production

Packaging and titration of herpes simplex virus 1 (HSV1) vectors were performed as reported previously (Alonso et al., 1998). Astrocyte cultures were infected with an MOI ranging between 0.01 and 0.1 one day before use.

### $Ca^{2+}$ Imaging

HeLa cell imaging was performed in a Nikon Diaphot inverted microscope using a 20× PlanApoUV objective (NA = 0.7, Olympus) as described previously (Villalobos et al., 1997). Briefly, standard medium containing 145 mM NaCl, 5 mM KCl, 1 mM $CaCl_2$, 1 mM $MgCl_2$, 10 mM glucose, and 10 mM Na-HEPES (pH 7.4), was applied at 22–25°C by perfusion at 5–6 ml/min. GAP was excited using the two filters, 403/12 DF and 470/25 DF, and a DM500 dichroic mirror. Cells were alternately epi-illuminated at 403 and 470 nm, and light emitted above 520 nm was recorded using a Hamamatsu C4742-98 camera handled by the Simple PCI 6.6 Hamamatsu software. For simultaneous recording of $[Ca^{2+}]_{ER}$ and $[Ca^{2+}]_C$, erGAP-expressing cells were incubated for 60 min with Rhod-3 AM (2 μM; Molecular Probes) at 22°C (Figure 1D). Cells were imaged in a Zeiss Axioplan upright microscope equipped with a 20× objective (W-Achroplan, Zeiss; NA = 0.5), sequentially excited at 405, 470, and 540 nm, and fluorescence was read at >515 (535DF35) nm and >590 (LP590) nm. The background was subtracted from the output images and pixel-to-pixel ratios were calculated using ImageJ software. The ratio $F_{470}/F_{403}$ was used as an index of

$[Ca^{2+}]_{ER}$ and $F_{540}$, generally expressed as $F/F_0$, as an index of $[Ca^{2+}]_C$. $F_0$ was the average of the fluorescence values obtained during the first 5–10 frames. $[Ca^{2+}]_C$ was also measured using Fura-2 (Figure S2B) as described previously (Rodriguez-Garcia et al., 2014). Astrocyte imaging was performed similarly.

### Generation of Transgenic Mice

Animal maintenance and handling were carried out in accordance with institutional regulations and guidelines and approved by the animal care committee of the University of Valladolid. The 5 kb transgene (Figure S3A) containing either the erGAP2 or the erGAP3 gene was injected into C57BL/6JCrl (Charles Rivers) or B6CBAF2/OlaHsd (Harlan) oocytes, respectively, using standard techniques. Genotyping was routinely performed by PCR of genomic DNA obtained from tail biopsies using four oligonucleotides, 30 and 31 (Supplemental Experimental Procedures) for GAP (234 bp product), together with 32 and 33 for endogenous *glyceraldehyde 3-phosphate dehydrogenase* (*gapdh*), a housekeeping gene (350 bp product). Experiments shown here were performed with mice of line 3 for erGAP2 and lines 1 and 10 for erGAP3. Experiments conformed to the institutional and national regulatory standards concerning animal welfare.

### Calcium Imaging in Brain Slices

Acute hippocampal slices were prepared from mice (P7-P15) from transgenic lines erGAP2 (L3) or erGAP3 (L1 or L10). The hippocampus was dissected out along with the cortex and sliced into 350–400 μm thick sections with a McIlwain Tissue Chopper. Slices were quickly transferred to a fine-meshed membrane filter and maintained in artificial cerebrospinal fluid (ACSF) containing: 125 mM NaCl, 2.5 mM KCl, 1 mM $MgCl_2$, 26 mM $NaHCO_3$, 1 mM $CaCl_2$, 10 mM glucose, and 1.25 mM $NaH_2PO_4$ (pH 7.4), continuously bubbled with a 95% $O_2$/5% $CO_2$ gas mixture at 25°C. Slices were mounted onto the stage of a Zeiss Axioplan upright microscope equipped with a 5× objective (Plan-Neofluar, Zeiss; NA = 0.15) and a Zeiss AxioCam camera MRm (12 bit) connected through a software interface (Axiovision, Zeiss) to a xenon fluorescent excitation source and a filter wheel. GAPs were excited at 405 and 470 nm and acquired at 518–553 nm, as described above. For simultaneous measuring of $[Ca^{2+}]_{ER}$ and $[Ca^{2+}]_C$, slices were incubated for 1 hr at room temperature with 16 μM Rhod-3 AM in bubbled ACSF medium. Imaging was performed as described above for HeLa cells. All the experiments were performed at 22°C–25°C in a custom-made chamber of 42 μl volume under constant perfusion at 3 ml/min.

### Generation of Transgenic Flies

PhiC31 system-mediated (Bischof et al., 2007) transformation of *Drosophila melanogaster* strain "$y^1$ M{vas-int.Dm}ZH-2A w*; M{3xP3-RFP.attP} ZH-86Fb" (BL24749) was used. *pUASTattB-erGAP3* was injected into embryos and stable lines with the transgene incorporated into an *attP86* site on the third chromosome were selected (BestGene). We used the Gal4-UAS system (Brand and Perrimon, 1993) to express erGAP3 in muscle cells. *UAS-erGAP3* or *UAS-GCaMP3* flies (Tian et al., 2009) were crossed with myosin heavy chain (*Mhc*)-Gal4 flies (Schuster et al., 1996).

### Calcium Imaging in Flies

Adult *Drosophila* were anesthetized with $CO_2$, tethered ventrally with a small drop of agar and then gently transferred to the microscope stage. Recordings of the dorsal longitudinal muscles in the fly thorax were obtained by stimulation of the giant fiber system through two tungsten electrodes impaled into the fly eyes (Allen and Godenschwege, 2010). The stimulation protocol consisted of voltage stimuli of 5–10 V and 30–50 ms duration at different frequencies (0.25–16 Hz). Each experiment started with a visual check of twitches in the wing after stimulation. Fluorescence images were acquired with a Leica MZ16FA fluorescence stereo microscope equipped with a Plan Apo 1.0× objective (NA = 0.14) and a 100 W mercury lamp, using either 470/40 nm or 405/40 excitation filters and a 525/50 nm emission filter. Images were acquired at 12 bits with binning of 2 × 2 or 4 × 4 and a zoom of 6.5×.

### Statistical Analysis

Results are expressed as means ± SD or means ± SEM, as indicated. The statistical significance was evaluated using Student's t test or one-way ANOVA with GraphPad InStat3 software.

## ACCESSION NUMBERS

The sequence of erGAP3 has been deposited in GenBank (KX181639) and in Addgene (78118).

## SUPPLEMENTAL INFORMATION

Supplemental Information includes Supplemental Experimental Procedures, four figures, and two movies and can be found with this article online at http://dx.doi.org/10.1016/j.chembiol.2016.05.010.

## AUTHOR CONTRIBUTIONS

J.G.-S. and M.T.A. conceived and designed the study. M.T.A. was responsible for molecular biology designs. L.L.L. helped with the design of the low-affinity mutations for $Ca^{2+}$. M.D.G. helped with the design and execution of the experiments in flies. P.N.-N., J.R.-R., and M.R.-P. performed the experiments and analyzed the data. J.G.-S. and M.T.A. wrote the manuscript. J.G.-S. supervised the whole study. All authors discussed the conceptual and practical implications of the results.

## ACKNOWLEDGMENTS

We thank M. García for technical assistance; I. López, Y. Gaciño, and F. Martínez for assistance with mice; A. Martín for assistance with cell sorting; J. Fernández, C. Lázaro, and R. Pascua-Maestro for help with flies; M. Torres and L.M. Criado for mouse microinjections; and, P. Chamero and T. Schimmang for suggestions on the manuscript. We thank A. Ferrús (Instituto Cajal, Madrid, Spain) for providing *Mhc*-Gal4 flies. Preliminary recordings in *Drosophila* were performed by medical student J. González Zamora. This work was supported by grants from the Spanish Ministerio de Economia y Competitividad (BFU2014-53469P) and the Instituto de Salud Carlos III (TerCel; RD16/0011/0003).

Received: March 17, 2016
Revised: May 5, 2016
Accepted: May 10, 2016
Published: June 9, 2016

## REFERENCES

Alonso, M.T., and Garcia-Sancho, J. (2011). Nuclear Ca(2+) signalling. Cell Calcium *49*, 280–289.

Alonso, M.T., Barrero, M.J., Carnicero, E., Montero, M., Garcia-Sancho, J., and Alvarez, J. (1998). Functional measurements of [Ca2+] in the endoplasmic reticulum using a herpes virus to deliver targeted aequorin. Cell Calcium *24*, 87–96.

Alonso, M.T., Barrero, M.J., Michelena, P., Carnicero, E., Cuchillo, I., Garcia, A.G., Garcia-Sancho, J., Montero, M., and Alvarez, J. (1999). Ca2+-induced Ca2+ release in chromaffin cells seen from inside the ER with targeted aequorin. J. Cell Biol. *144*, 241–254.

Allen, M.J., and Godenschwege, T.A. (2010). Electrophysiological recordings from the *Drosophila* giant fiber system (GFS). Cold Spring Harb. Protoc. *2010*, pdb prot5453.

Aulestia, F.J., Alonso, M.T., and Garcia-Sancho, J. (2015). Differential calcium handling by the cis and trans regions of the Golgi apparatus. Biochem. J. *466*, 455–465.

Bakayan, A., Vaquero, C.F., Picazo, F., and Llopis, J. (2011). Red fluorescent protein-aequorin fusions as improved bioluminescent Ca2+ reporters in single cells and mice. PLoS One *6*, e19520.

Bischof, J., Maeda, R.K., Hediger, M., Karch, F., and Basler, K. (2007). An optimized transgenesis system for *Drosophila* using germ-line-specific phiC31 integrases. Proc. Natl. Acad. Sci. USA *104*, 3312–3317.

Brand, A.H., and Perrimon, N. (1993). Targeted gene expression as a means of altering cell fates and generating dominant phenotypes. Development *118*, 401–415.

Csordas, G., Varnai, P., Golenar, T., Roy, S., Purkins, G., Schneider, T.G., Balla, T., and Hajnoczky, G. (2010). Imaging interorganelle contacts and local calcium dynamics at the ER-mitochondrial interface. Mol. Cell *39*, 121–132.

Dallwig, R., Vitten, H., and Deitmer, J.W. (2000). A novel barium-sensitive calcium influx into rat astrocytes at low external potassium. Cell Calcium *28*, 247–259.

Fernandez-Santiago, R., and Ezquerra, M. (2016). Epigenetic research of neurodegenerative disorders using patient iPSC-based models. Stem Cells Int. *2016*, 9464591.

Fernandez de Sevilla, D., Nunez, A., Borde, M., Malinow, R., and Buno, W. (2008). Cholinergic-mediated IP3-receptor activation induces long-lasting synaptic enhancement in CA1 pyramidal neurons. J. Neurosci. *28*, 1469–1478.

Gallego-Sandin, S., Alonso, M.T., and Garcia-Sancho, J. (2011). Calcium homoeostasis modulator 1 (CALHM1) reduces the calcium content of the endoplasmic reticulum (ER) and triggers ER stress. Biochem. J. *437*, 469–475.

Giacomello, M., Drago, I., Bortolozzi, M., Scorzeto, M., Gianelle, A., Pizzo, P., and Pozzan, T. (2010). Ca2+ hot spots on the mitochondrial surface are generated by Ca2+ mobilization from stores, but not by activation of store-operated Ca2+ channels. Mol. Cell *38*, 280–290.

Henderson, M.J., Baldwin, H.A., Werley, C.A., Boccardo, S., Whitaker, L.R., Yan, X., Holt, G.T., Schreiter, E.R., Looger, L.L., Cohen, A.E., et al. (2015). A low affinity GCaMP3 variant (GCaMPer) for imaging the endoplasmic reticulum calcium store. PLoS One *10*, e0139273.

Kienzle, C., and von Blume, J. (2014). Secretory cargo sorting at the trans-Golgi network. Trends Cell Biol. *24*, 584–593.

Manjarres, I.M., Chamero, P., Domingo, B., Molina, F., Llopis, J., Alonso, M.T., and Garcia-Sancho, J. (2008). Red and green aequorins for simultaneous monitoring of Ca2+ signals from two different organelles. Pflugers Arch. *455*, 961–970.

Miyazaki, J., Takaki, S., Araki, K., Tashiro, F., Tominaga, A., Takatsu, K., and Yamamura, K. (1989). Expression vector system based on the chicken beta-actin promoter directs efficient production of interleukin-5. Gene *79*, 269–277.

Moore, G.A., Kass, G.E., Duddy, S.K., Farrell, G.C., Llopis, J., and Orrenius, S. (1990). 2,5-Di(tert-butyl)-1,4-benzohydroquinone–a novel mobilizer of the inositol 1,4,5-trisphosphate-sensitive Ca2+ pool. Free Radic. Res. Commun. *8*, 337–345.

Palmer, A.E., and Tsien, R.Y. (2006). Measuring calcium signaling using genetically targetable fluorescent indicators. Nat. Protoc. *1*, 1057–1065.

Power, J.M., and Sah, P. (2002). Nuclear calcium signaling evoked by cholinergic stimulation in hippocampal CA1 pyramidal neurons. J. Neurosci. *22*, 3454–3462.

Rodriguez-Garcia, A., Rojo-Ruiz, J., Navas-Navarro, P., Aulestia, F.J., Gallego-Sandin, S., Garcia-Sancho, J., and Alonso, M.T. (2014). GAP, an aequorin-based fluorescent indicator for imaging Ca2+ in organelles. Proc. Natl. Acad. Sci. USA *111*, 2584–2589.

Schuster, C.M., Davis, G.W., Fetter, R.D., and Goodman, C.S. (1996). Genetic dissection of structural and functional components of synaptic plasticity. I. Fasciclin II controls synaptic stabilization and growth. Neuron *17*, 641–654.

Shaner, N.C., Campbell, R.E., Steinbach, P.A., Giepmans, B.N., Palmer, A.E., and Tsien, R.Y. (2004). Improved monomeric red, orange and yellow fluorescent proteins derived from *Discosoma* sp. red fluorescent protein. Nat. Biotechnol. *22*, 1567–1572.

Suzuki, J., Kanemaru, K., Ishii, K., Ohkura, M., Okubo, Y., and Iino, M. (2014). Imaging intraorganellar Ca2+ at subcellular resolution using CEPIA. Nat. Commun. *5*, 4153.

Tang, S., Wong, H.C., Wang, Z.M., Huang, Y., Zou, J., Zhuo, Y., Pennati, A., Gadda, G., Delbono, O., and Yang, J.J. (2011). Design and application of a class of sensors to monitor Ca2+ dynamics in high Ca2+ concentration cellular compartments. Proc. Natl. Acad. Sci. USA *108*, 16265–16270.

Thastrup, O., Dawson, A.P., Scharff, O., Foder, B., Cullen, P.J., Drobak, B.K., Bjerrum, P.J., Christensen, S.B., and Hanley, M.R. (1989). Thapsigargin, a novel molecular probe for studying intracellular calcium release and storage. Agents Actions *27*, 17–23.

Tian, L., Hires, S.A., Mao, T., Huber, D., Chiappe, M.E., Chalasani, S.H., Petreanu, L., Akerboom, J., McKinney, S.A., Schreiter, E.R., et al. (2009). Imaging neural activity in worms, flies and mice with improved GCaMP calcium indicators. Nat. Methods *6*, 875–881.

Verkhratsky, A., Rodriguez, J.J., and Parpura, V. (2012). Calcium signalling in astroglia. Mol. Cell Endocrinol. *353*, 45–56.

Villalobos, C., Nunez, L., Frawley, L.S., Garcia-Sancho, J., and Sanchez, A. (1997). Multi-responsiveness of single anterior pituitary cells to hypothalamic-releasing hormones: a cellular basis for paradoxical secretion. Proc. Natl. Acad. Sci. USA *94*, 14132–14137.

Wan, W., Cao, L., Kalionis, B., Xia, S., and Tai, X. (2015). Applications of induced pluripotent stem cells in studying the neurodegenerative diseases. Stem Cells Int. *2015*, 382530.

Wu, J., Prole, D.L., Shen, Y., Lin, Z., Gnanasekaran, A., Liu, Y., Chen, L., Zhou, H., Chen, S.R., Usachev, Y.M., et al. (2014). Red fluorescent genetically encoded Ca2+ indicators for use in mitochondria and endoplasmic reticulum. Biochem. J. *464*, 13–22.